Homogeneous melting of metals with different crystalline structure

2006 J. Phys.: Condens. Matter 18 5639

(http://iopscience.iop.org/0953-8984/18/24/006)

INSTITUTE OF PHYSICS PUBLISHING JOURNAL OF PHYSICS: CONDENSED MATTER

J. Phys.: Condens. Matter **18** (2006) 5639–5653 doi:10.1088/0953-8984/18/24/006

Homogeneous melting of metals with different crystalline structure

F Delogu

Dipartimento di Ingegneria Chimica e Materiali, Università di Cagliari, piazza d'Armi, I-09123 Cagliari, Italy

E-mail: delogu@dicm.unica.it

Received 9 March 2006, in final form 13 April 2006
Published 2 June 2006
Online at stacks.iop.org/JPhysCM/18/5639

Abstract

Numerical simulations have been used to investigate the thermal response to a gradual temperature rise in surface-free bulks of metallic elements with different crystalline structure. The increase in thermal vibration amplitudes determines the appearance of atoms with defective coordination. Their number increases with temperature at a rate depending on the thermal properties of the crystalline lattice. Due to the absence of free surfaces and other structural defects, melting takes place at the first limit of superheating. Numerical findings point out that, at such a temperature, elements with the same crystallographic structure display roughly the same content of atoms with defective coordination. The fraction of defectively coordinated atoms at the homogeneous melting point is then a quantity characteristic of the crystalline lattice. The relationship between the homogeneous and the heterogeneous melting points is also discussed in the light of the different mechanisms underlying the melting processes.

(Some figures in this article are in colour only in the electronic version)

1. Introduction

Homogeneous melting takes place whenever the heterogeneous nucleation of the molten phase at defective lattice sites is suppressed [1–3]. Under such circumstances, the stability of the crystalline phase is limited by a hierarchy of entropy-, enthalpy-, volume- and rigidity-driven catastrophes with homogeneous mechanisms [4, 5]. The first limit to the stability of the crystal lattice is determined by the homogeneous nucleation of melting in the bulk [6].

In contrast to the heterogeneous melting process starting at surfaces and interfaces [2, 3], homogeneous melting initiates in excited bulk regions in which atomic displacements from equilibrium lattice positions locally induce the mechanical failure of the crystal [7] and determines the maximum limit of superheating, unless extremely high heating rates are applied [8]. It also points out a deep connection between the most venerated melting criteria

proposed by Lindemann and Born, based respectively on vibration- and phonon-induced crystal instabilities [5, 9, 10]. Other mechanistic studies focused on the appearance and interaction of atoms with defective coordination and demonstrated that homogeneous melting at the limit of superheating is a defect-mediated process [11–16]. The identification of dislocation lines and loops at relatively high temperatures [11–16] indeed establishes an interesting connection between numerical findings and theoretical models for a dislocation-mediated transition [2, 17]. In a sense, it also strengthens the hope that the comprehensive theoretical framework for the melting of two-dimensional systems proposed by Kosterlitz and Thouless [18], Nelson and Halperin [19] and Young [20] could be extended to three-dimensional systems.

This work gives a further contribution along such a line of inquiry by investigating the homogeneous melting behaviour of metals with different crystalline structures in order to ascertain the role of the lattice geometry. The number of atoms with defective coordination as well as of their aggregates in surface-free bulks of 11 metallic species were estimated by means of molecular dynamics simulations. A comparison between homogeneous and heterogeneous melting processes is also carried out. Numerical methods are outlined in the following.

2. Molecular dynamics simulations

Calculations were carried out on metals with face-centred cubic (fcc), hexagonal close-packed (hcp) and body-centred cubic (bcc) crystalline structures. The fcc elements that were considered were Ag, Al, Au, Cu and Ni. These five metallic species have been the subject of recent work [12, 13]. Part of the published data will be reproduced here for the sake of comparison. Four systems with hcp structure, namely Mg, Ti, Zn and Zr, and two metals, Mo and V, with a bcc lattice have been also considered. However, it is worth noting that Ti and Zr undergo a hcp-to-bcc phase transition at high temperatures. Therefore, although starting with an hcp arrangement, the homogeneous melting process of Ti and Zr involves a bcc structure [21].

2.1. Interatomic potentials

The interatomic potentials for metallic species with initial fcc and hcp structures were described within the framework of the second-moment approximation of the tight-binding (TB) band energy [22–24]. The potential parameter values that are characteristic of each chemical species were taken from the literature [24]. Interactions were computed within a cut-off radius that roughly corresponds to the distance of the seventh neighbours' shell. Unfortunately, the TB potential is not able to stabilize the bcc geometry satisfactorily [24]. In particular, the hcp and fcc structures are always more stable than the bcc structure. Correspondingly, simulations employing TB interactions for bcc metals unavoidably result in a gradual transformation from the bcc lattice to either the hcp or the fcc lattices [24]. For these reasons, in the case of bcc metals the interactions were reproduced with a Finnis–Sinclair (FS) potential [25]. The FS approach describes the many-body forces between atoms of bcc elements in terms of a TB approximation. However, it provides a potential that is mathematically equivalent to the one obtained with the embedded-atom method (EAM) [26, 27], which is based on a local electronic density functional theory. An appropriate choice of the characteristic parameters allows for the FS potential to guarantee adequate stability of the bcc lattice against any phase transformation into the hcp and fcc lattices [24–26]. As in the previous cases, the FS potential parameter values for Mo and V were taken from the literature [28, 29]. Also in these cases, interatomic forces were computed within a cut-off radius that roughly extends to the seventh neighbours.

It is worth noting here that the interactions have been extended to the larger possible number of coordination shells consistent with the available computational resources. The

response of the systems to such a cut-off extension has been tested in ad hoc simulations. These pointed out that thermodynamic properties were not significantly affected, being rather insensitive to the cut-off radius, provided that a certain threshold value is exceeded [24]. The mechanical stability of the crystalline lattice was instead improved and the uncertainties on the elastic constant values were lowered to about the 5%. Taking into account that mechanical properties play an important role in the homogeneous failure of the crystalline lattice, the extended cut-off distance permits a more reliable estimate of the homogeneous melting point.

The equations of motion were solved with a fifth-order predictor–corrector algorithm [30] and a time step δt of 2 fs.

2.2. Homogeneous melting

The first limit of superheating, $T_{\mathrm{m}}^{\mathrm{K}}$, was evaluated by sampling the *NPT* ensemble with the number of atoms N, pressure P and temperature T constant [31, 32]. Periodic boundary conditions (PBCs) were applied in the three Cartesian directions to simulate surface-free crystalline bulks. In the case of fcc metals [12, 13], computations were carried out on systems of 6912 atoms arranged in the fcc cF4 crystalline lattice within a cubic simulation box with 12 elementary crystallographic units per side. The crystalline bulks of hcp metals consisted instead of 6750 atoms defining a lattice with the hP2 geometry and located within a parallelepipedic box having 15 elementary crystallographic cells per side. The hcp cell is characterized by the two conventional parameters a and c indicating, respectively, the side length and the height of the crystallographic unit [33]. The so-called axial ratio c/a is a parameter that is characteristic of the hcp elements and is essentially determined by the nature and strength of the atomic-scale interactions [34]. The systems in the present work have been selected in order to have different axial ratios. In particular, the axial ratio of Zn, amounting to 1.856, is significantly higher than those pertaining to Mg, Ti and Zr, amounting respectively to 1.623, 1.587 and 1.592 [21, 24]. Calculations on bcc metals were performed on systems of 6750 atoms arranged within a cubic simulation box having 3375 elementary cells with bcc cI2 geometry per side.

The systems were initially relaxed at a temperature $T = 300$ K and an external pressure $P \approx 0$ for 1×10^5 time steps. Starting from 300 K, the equilibrated systems were gradually heated by increasing the temperature by 25 K every 2×10^4 time steps of relaxation. The long-range crystalline order was monitored by means of the pair correlation function (PCF) and the static order parameter $S(k)$ [12, 13, 29, 35, 36]. The latter allows for the reliable identification of the homogeneous melting point. At melting, the $S(k)$ values indeed undergo a sudden downward jump from about 0.7–0.8, typical of a thermally disordered crystalline phase, to 0.1–0.2, characteristic instead of an isotropic liquid [30, 35, 36]. The reciprocal space vector k was given suitable component values to monitor the crystalline order along the [111] crystallographic directions.

2.3. Crystalline order

The number and nature of structural defects were evaluated by looking at the atoms, hereafter referred to as defectively coordinated, with a coordination number different from the equilibrium one. For the fcc, hcp and bcc systems, the number of nearest neighbours at equilibrium amounts to 12, 12 and 8, respectively. The number of nearest neighbours was estimated by applying a distance criterion according to which two atoms are nearest neighbours whenever their distance is shorter than the distance, r_{min}, corresponding to the first minimum of PCF [11–14, 37]. This means that the extension of the coordination shell of a given atom is defined by the first peak of the PDF. Given that the systems are solid, the PCF peaks related

to the first and the second nearest-neighbours' shells can be distinguished well. As usual, the boundary between the two shells is identified with the distance $r_{\min}$ at which the PCF has its first minimum. Any given atom then has its nearest neighbours within a distance $r_{\min}$ and the total number of neighbours can be evaluated easily.

The same distance criterion also permits us to evaluate the degree of clustering of defectively coordinated atoms, i.e. the tendency to form aggregates. Two defectively coordinated atoms are thus regarded as belonging to the same cluster whenever their distance is shorter than $r_{\min}$ [11–14]. This allows for estimation of the number, N_{cl}, and the size, n, of the clusters.

It is worth noting here that the evaluation of the number, size and configurations of clusters is a necessary condition to investigate the role of lattice defects in the mechanism of homogeneous melting. The fact that a certain atom could be defectively coordinated indeed does not imply that such an atom necessarily corresponds or is part of either a point or a linear lattice defect. Actually, lattice defects can be identified only indirectly by means of defectively coordinated atoms. In particular, a lattice defect has to be characterized in terms of the configuration of defectively coordinated atoms. An example is provided by the case of a vacancy in a perfect fcc crystalline lattice. The atoms here are normally surrounded by 12 nearest neighbours. The vacant site is therefore also surrounded by 12 nearest neighbours. However, each atom neighbouring the vacancy possesses only 11 nearest neighbours due to the presence of the vacant site in its coordination shell. A vacancy is therefore associated with the configuration of 12 neighbouring atoms with 11 nearest neighbours each. Analogous reasoning can be followed for interstitials, identified by configurations of 12 neighbouring atoms with 13 nearest neighbours each. The situation for dislocations is instead different, given that their geometrical properties are strictly connected with the lattice topology, and their identification requires an estimation of Burgers' circuits.

Analysis of the local crystalline order was carried out by means of the so-called Honeycutt–Andersen (HA) parameters, which permit us to identify the local structural arrangement on the basis of the distances between atomic pairs in coordination shells [37].

The fraction $\alpha_{\mathrm{d}}(T)$ of defectively coordinated atoms, defined as the ratio between the number of defectively coordinated atoms and the total number of atoms in the system, and the total number N_{cl} of clusters were used to compare properly the behaviour of systems of different nature and size.

2.4. Heterogeneous melting point

The methodology employed to simulate heterogeneous melting is based on previous work [35, 36, 38, 39], and full details can be found elsewhere [40]. The heterogeneous melting process was not studied systematically for all the metallic species previously considered. Computations were carried out for the fcc systems, for hcp Zn, and for bcc Mo. Calculations were performed on systems consisting of a stacking of 48 (110) atomic planes along the z Cartesian direction terminating with a free surface, with each plane containing 144 atoms. PBCs were applied only along the x and y Cartesian directions. A reservoir region of five atomic planes was defined at the bottom of the simulation cell. Reservoir atoms were given fixed positions corresponding to a perfect fcc, hcp or bcc lattice. The top of the simulation cell consisted of an empty space, with a height corresponding to about ten atomic planes and bounded by a reflective barrier, which permits surface atoms to eventually sample the vapour phase.

The system described above was prepared by starting from a larger configuration of 58 fully equilibrated (110) atomic planes with PBCs applied along the x and y Cartesian directions

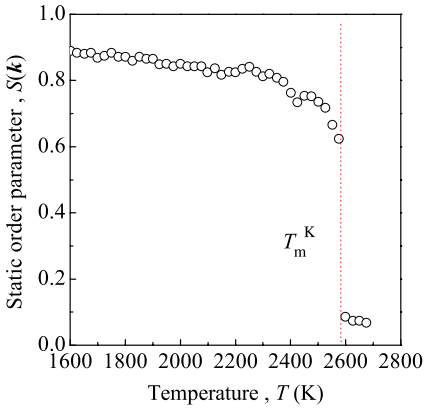

Figure 1. The static order parameter $S(k)$ as a function of the temperature T. A sudden drop in $S(k)$ values is observed at 2575 K, which marks the limit of superheating T_m^K at which the homogeneous melting occurs. Data refer to bcc V. Analogous trends are displayed by the other metallic species.

and two reservoir regions of five atomic planes along the z Cartesian direction, respectively at the top and at the bottom of the simulation cell. The relaxed free surface was generated by gradually canceling the pair interactions between the atoms belonging to the 48 (110) planes selected starting from the bottom and the remaining ones. Such a cancellation was performed by reducing the potential parameters A and ξ to zero in 1000 time steps. The resulting semi-crystal terminating with a free surface was further relaxed for 1×10^5 time steps at a temperature of 300 K and an external pressure $P \approx 0$ [40].

The degree of structural order and the collapse of the crystalline structure at the equilibrium melting point T_m were monitored plane-by-plane by means of the planar static order parameter $S_p(k)$, which is the two-dimensional analogue of $S(k)$ [30].

3. Numerical findings

The thermal response of the crystalline lattice to the gradual temperature rise is the same for all the chemical systems investigated. The amplitude of atomic vibrations around equilibrium lattice positions increases with temperature, determining an increasing disorder for the crystalline structure. The displacement of atoms from their equilibrium sites is readily pointed out by the static order parameter $S(k)$, which correspondingly undergoes a gradual decrease.

As shown in figure 1 for the case of V, the decrease in $S(k)$ values is approximately linear within a broad temperature range. Subsequently, the trend becomes markedly curved, and finally the gradual change is replaced by a sudden drop, pointing out a loss of structural order. The failure of the crystalline lattice takes place uniformly in the system [7, 11–14, 35, 36], and the temperature at which the static order parameter $S(k)$ drops to values close to zero corresponds to the homogeneous melting point T_m^K. The T_m^K values obtained for the 11 metallic species considered are reported in table 1.

The value of the homogeneous melting point T_m^K is sensitive to the size of the simulated system. Size effects have been investigated on Al and Cu fcc systems consisting of 864, 2048, 4000, 6912 and 10 976 atoms, respectively, as well as on Mo bcc systems containing 1024, 3456, 6750 and 11 664 atoms. The results obtained in the case of Al are shown for the sake

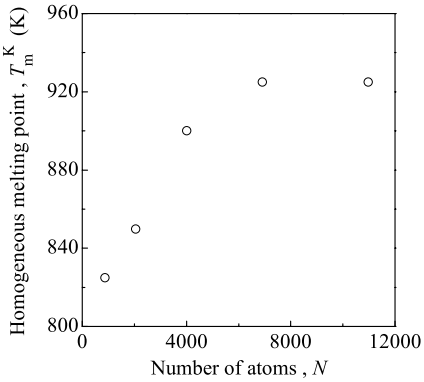

Figure 2. The limit of superheating, T_m^K, as a function of the number N of atoms in the system. It can be seen that size effects significantly affect the smallest systems. Data refer to fcc Al. Analogous trends are displayed for fcc Cu and bcc Mo, and are expected for the other metallic species.

Table 1. Numerical estimates of the equilibrium melting point T_m and of the limit of superheating T_m^K.

Element	T_m^K (K)	T_m (K)
Ag	1250	1000
Al	925	775
Au	1400	1150
Cu	1650	1275
Mg	1050	910[c]
Mo	3375	2850
Ni	2025	1700
Ti	2275	1750[a]
V	2575	2220[b]
Zn	850	700
Zr	2375	1875[a]

[a] Values taken from [12].
[b] Value taken from [29].
[c] Value obtained from interpolation.

of illustration in figure 2, where the T_m^K values are quoted as a function of the total number N of atoms in the system. The numerical findings indicate that the system size significantly affects the behaviour of the smallest systems, i.e. those containing 864 and 2048 atoms in the case of fcc metals and that with 1024 atoms in the case of Mo. Similar T_m^K values are instead obtained in the remaining cases. The results obtained for Al and Cu indicate that the values of the observables that are taken into account change on average by only 3% when the number of atoms changes from 4000 to 10 976. Analogously, the values obtained for Mo change by 3% when the number of atoms changes from 3456 to 11 664. These results point out a satisfactory robustness of the simulated systems against size effects. Accordingly, the results arising from the systematic investigations carried out on fcc, hcp and bcc systems of 6912, 6750 and 6750 atoms, respectively, can be considered to be meaningful.

The thermal behaviour of systems terminating with a free surface is analogous to the behaviour described above. The values of the planar static order parameter $S_p(k)$ undergo a gradual decrease as the temperature increases for all the atomic planes, except for those in the reservoir region that contains immobile species. The gradual decrease is followed at a certain

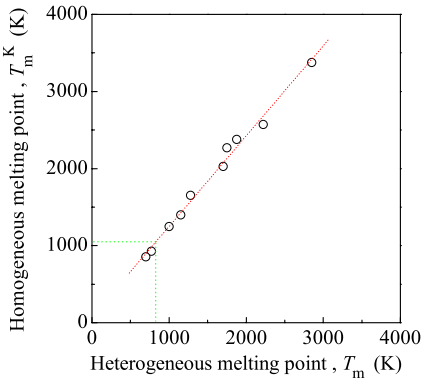

Figure 3. The homogeneous melting point T_m^K as a function of the equilibrium melting point T_m. A linear trend is observed. The best-fitted line is also shown. The horizontal dotted lines mark the T_m^K value of the hcp Mg and the vertical dotted line identifies the corresponding T_m estimate.

temperature by a sudden downward jump to values that are characteristic of the liquid phase. Although dependent on the topology of the free surface, its value changing as the Miller indices change, such a temperature represents a satisfactory estimate of the equilibrium melting point, T_m [35, 36, 38, 40]. In all the cases, melting starts at the free surface and then propagates to the bulk [40]. The T_m values obtained for the fcc metals as well as those for hcp Zn and bcc Mo are also reported in table 1.

Estimates of the melting points T_m of Ti and Zr metals, obtained using a TB semi-empirical potential but a different methodology, also exist [12] and have been reported in the table. Finally, the estimate of the T_m value for the bcc V, also quoted in table 1, was taken from the literature [29]. It appears then that the unique element for which an estimate of the equilibrium melting point T_m is not available is hcp Mg. However, such an estimate can likewise be obtained even without additional simulations by taking into account the relationship between the homogeneous melting point T_m^K and the heterogeneous melting point T_m. It is indeed worth noting that the T_m^K values arrange according to an approximately linear trend when quoted as a function of the corresponding T_m values, as in figure 3. It is also worth noting that the linear trend involves all the melting points, irrespective of the structure of the elemental species for which they are characteristic. This means that a deep connection exists between homogeneous and heterogeneous melting, in accordance with theoretical predictions [6].

The mechanism of homogeneous melting has been characterized in detail for all the metallic species by quantifying the numbers of defective atoms and of their clusters. For the sake of clarity, the cases of fcc, hcp and bcc metals will be discussed separately.

3.1. Elements with fcc structure

The fraction $\alpha_d(T)$ of defectively coordinated atoms for the fcc metals is shown in figure 4(a) as a function of temperature T. The species display analogous trends, monotonically increasing with temperature. The increase is linear in the first portion of the plot, but becomes markedly curved as the limit of superheating, T_m^K, is approached. The different curves in figure 4(a) superpose when plotted as a function of the reduced temperature T/T_m^K. This indicates that the homogeneous melting point T_m^K is a scaling factor for the fraction $\alpha_d(T)$ of defectively coordinated atoms. The superposed plots in figure 4(b) also point out the similarity of the $\alpha_d(T_m^K)$ values at the homogeneous melting point T_m^K, amounting to about 0.4 in all the cases.

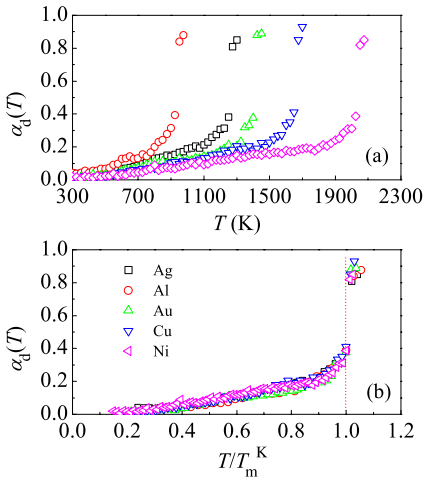

Figure 4. The fraction $\alpha_d(T)$ of defectively coordinated atoms as a function of (a) the temperature T and (b) the reduced temperature T/T_m^K. The curves in (b) superpose, indicating that T_m^K is a scaling factor for $\alpha_d(T)$. In all cases, the $\alpha_d(T_m^K)$ value at the homogeneous melting point T_m^K amounts to about 0.4.

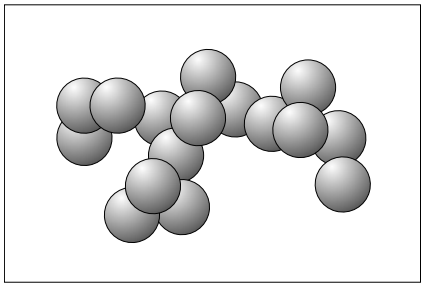

Figure 5. A small cluster of 16 defectively coordinated atoms of Au at 1200 K.

At relatively low temperatures, the rearrangement of coordination shells determines the formation of isolated defectively coordinated atom pairs. However, the degree of cooperation of such processes increases with temperature, inducing the formation of aggregates of defectively coordinated atoms such as those shown in figure 5.

The number N_{cl} of defectively coordinated atom clusters for the different chemical species is quoted in figure 6 as a function of the reduced temperature T/T_m^K. The data superposition indicates that T_m^K represents a scaling factor for the processes underlying the appearance and interaction of defectively coordinated atoms. Figure 6 shows, in addition, that the number N_{cl} of clusters has a strong dependence on the temperature. It can be seen that N_{cl} first undergoes a smooth increase, then attains a maximum value at about 0.8 T_m^K and finally decreases. The observed non-monotonic trend can be explained by the competition between ramification, fragmentation and coalescence events affecting the number, the size and the shape of clusters [11–14]. Ramification and fragmentation processes are related to the number of defectively coordinated atoms and initially predominate, determining an increase in the number of clusters due to the increase in the content of defectively coordinated atoms. However, ramification events also determine the increase in the cluster size n, i.e. of the number of defectively coordinated atoms connected in a given cluster. Given that the space occupied by a

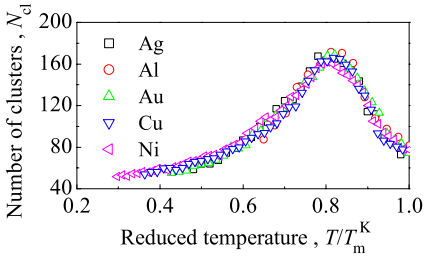

Figure 6. The number N_{cl} of clusters of defectively coordinated atoms as a function of the reduced temperature T/T_m^K. A maximum at about 0.8 T_m^K is observed.

cluster is roughly proportional to its size, the increase in the cluster size gradually favours the occurrence of coalescence events between the defectively coordinated atom aggregates. This finally results in a significant decrease in the total number N_{cl} of clusters [11–14].

Small clusters consisting of about 10 atoms display approximately linear configurations, forming string-like structures [11–14]. These clusters, which are relatively abundant at low temperatures, have been regarded as pseudo-dislocations or, alternatively, as dislocation cores [15, 16]. However, it must be pointed out that such small clusters only rarely display properties characteristic of dislocations. As the average size of clusters increases, the probability that a given cluster possesses the characteristic of dislocation loops and lines increases [12, 13]. Shockley partial dislocations with a (111) glide plane moving irregularly in the [110] and one of the [211] crystallographic directions have been observed at relatively high temperatures. Open dislocation lines with a (111) glide plane crossing the whole system have occasionally been detected in the temperature range close to the limit of superheating. Similarly, smaller configurations of 12 neighbouring atoms with either 11- or 13-fold coordination revealed the formation of vacancies and interstitials, respectively [12, 13]. Of course, the number of lattice defects is considerably smaller than the number of defectively coordinated atoms, and the fraction of interstitials and vacancies in fcc, hcp and bcc lattices has a value of about 10^{-5}–10^{-4}. These results are then satisfactorily close to the experimental results. Analysis of the local crystalline order with the HA parameters indicates that the dislocations, as well as the other defectively coordinated atom aggregates, are related to the formation of stacking faults consisting of crystalline domains of about 30–40 atoms with an hcp arrangement.

3.2. Elements with hcp structure

The melting behaviour of the Mg and Zn hcp systems is expected to be relatively similar to the behaviour displayed by fcc elements, due to the fact that both the hcp and fcc structures are close-packed, their differences originating from the different alternate stacking of (111) planes. The fractions $\alpha_d(T)$ of defectively coordinated atoms for Mg and Zn are reported in figure 7(a) as a function of the reduced temperature T/T_m^K. The two curves, displaying a monotonic increase, are superposed. It can be seen that the $\alpha_d(T_m^K)$ values amount again to about 0.4. The critical fraction $\alpha_d(T_m^K)$ of defectively coordinated atoms at the limit of superheating T_m^K then takes approximately the same value for fcc and hcp elements, thus suggesting that these species have an analogous mechanism of homogeneous melting.

The defectively coordinated atoms appear and interact in the surface-free bulk of hcp species with the same dynamics shown in the case of fcc elements. Defectively coordinated atom pairs isolated at relatively low temperatures become connected as the temperature

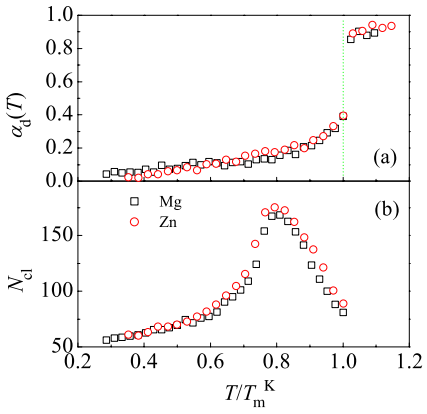

Figure 7. The fraction $\alpha_d(T)$ of defectively coordinated atoms (a) and the number N_{cl} of clusters of defectively coordinated atoms (b) as a function of the reduced temperature T/T_m^K. The curves are analogous to those for fcc metals.

increases, as a consequence of the rearrangement of coordination shells. The defectively coordinated atoms form clusters similar to that depicted in figure 3. The number, N_{cl}, of such clusters is shown in figure 7(b) as a function of the reduced temperature T/T_m^K. The superposed curves display a non-monotonic trend, analogous to the one displayed by fcc elements in figure 6. However, it appears that the N_{cl} values of Zn are slightly higher than those for Mg.

The clusters of defectively coordinated atoms formed in the hcp lattices have apparently the same shape and configuration as those observed in the fcc lattices. Again, the small string-like clusters detected at relatively low temperatures interact with each other and are gradually replaced by larger ones as the temperature rises. The dislocation lines and loops occasionally observed at temperatures close to T_m^K mostly have a (001) glide plane and move in the [100] crystallographic direction. Vacancy–interstitial complexes, as well as isolated vacancies and interstitials, have also been observed. The HA parameters point out the formation of stacking faults and the consequent appearance of crystalline regions of about 20–30 atoms having either fcc or bcc local order.

3.3. Elements undergoing the hcp-to-bcc phase transition

The allotropic phase of Ti and Zr stable at relatively low temperatures is the hcp phase [21]. However, both Ti and Zr undergo a hcp-to-bcc phase transition, observed experimentally at about 1100 K [21]. The atomic-scale mechanism governing such a structural transition has been studied in detail in the past for Zr [41] and will not be dealt with here in order to keep the focus on the role of defectively coordinated atoms in the homogeneous melting processes.

The fraction $\alpha_d(T)$ of defectively coordinated atoms for Ti and Zr is shown in figure 8(a) as a function of the reduced temperature T/T_m^K. The superposition between the increasing monotonic curves of the two elements is almost perfect. The content of defectively coordinated atoms increases according to a roughly linear trend up to a temperature of about 1800 K. At such a temperature, the superposed curves display a discontinuity consisting of a sudden increase. More specifically, the increase takes place at 1800 K for Ti and at 1850 K for Zr. The HA parameters reveal that, at temperatures close to but lower than those mentioned above, the fractions $\alpha_{Ti,bcc}$ and $\alpha_{Zr,bcc}$ of Ti and Zr atoms with a bcc crystalline environment are on the order of 0.1. At 1800 K for Ti and at 1850 K for Zr, the HA analysis indicates that the local

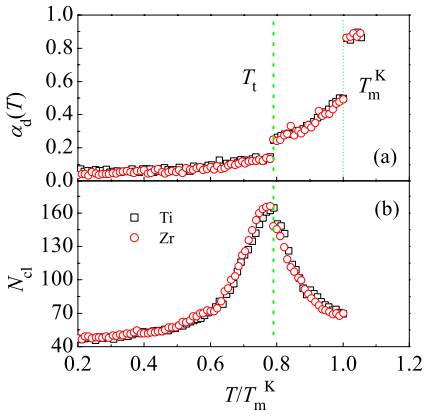

Figure 8. The fraction $\alpha_d(T)$ of defectively coordinated atoms (a) and the number N_{cl} of clusters of defectively coordinated atoms (b) as a function of the reduced temperature T/T_m^K. The curves are characterized by a discontinuity at about 0.8 T_m^K, which identifies the hcp-to-bcc transition temperature T_t. At such a temperature, $\alpha_d(T)$ and N_{cl} undergo a sudden increase and decrease, respectively.

crystalline order changes drastically. The fractions $\alpha_{Ti,bcc}$ and $\alpha_{Zr,bcc}$ of Ti and Zr atoms with a bcc crystalline environment are indeed found to amount to about 0.85. The discontinuities in the values of the fraction $\alpha_d(T)$ of defectively coordinated atoms then mark the occurrence of the hcp-to-bcc phase transition, and the temperatures mentioned above correspond to the transition temperature T_t.

The phase transformation mechanism, which is expected to be the same for the two metals, involves anisotropic contraction and extension processes of atomic planes of the hcp lattice along given crystallographic directions [41]. Mechanistic features will not be discussed here in detail, for the sake of brevity and clarity. However, it is worth noting that the transition temperatures observed for Ti and Zr, although considerably higher than the experimental values [21], are in substantial agreement with the transition temperature observed in previous simulation work with the TB force scheme [41]. The slightly lower transition temperatures obtained in the present work are related to a different choice of potential parameters, as well as to different simulations conditions [21, 41].

As is evident from figure 8(a), at temperatures higher than T_t, the fraction $\alpha_d(T)$ of defectively coordinated atoms again undergoes a smooth increase. It is worth remembering here that the crystalline structures of Ti and Zr now have a bcc geometry, so that the homogeneous melting process concerns a structural arrangement that is not close-packed. This aspect probably makes less surprising the observation that the $\alpha_d(T_m^K)$ values at the homogeneous melting point T_m^K for Ti and Zr are significantly different from those observed in the cases of the elements melting with fcc and hcp structures. In particular, Ti and Zr display $\alpha_d(T_m^K)$ values on the order of 0.5, whereas, in all the other cases discussed hitherto, the fraction $\alpha_d(T_m^K)$ of defective atoms was equal to about 0.4.

The transition from the hcp to the bcc structure also affects the total number N_{cl} of defectively coordinated atom clusters. The data in figure 8(b), where N_{cl} is quoted as a function of the reduced temperature T/T_m^K, show that the trend is initially similar to those for fcc and hcp elements. However, discontinuities in the number N_{cl} of clusters are evident at T_t for Ti and Zr. In this case, the discontinuities are marked by a sudden decrease in the number N_{cl} of clusters. This is a consequence of the definite increase undergone by the fraction $\alpha_d(T)$

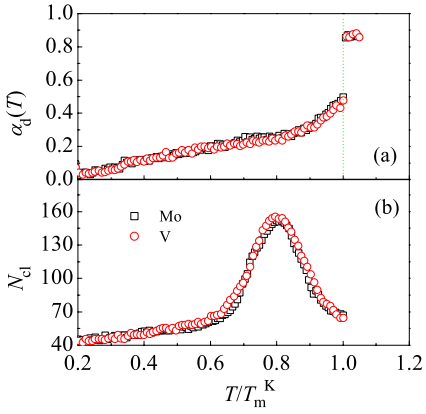

Figure 9. The fraction $\alpha_d(T)$ of defectively coordinated atoms (a) and the number N_{cl} of clusters of defectively coordinated atoms (b) as a function of the reduced temperature T/T_m^K. The fraction $\alpha_d(T_m^K)$ of defectively coordinated atoms at melting amounts to about 0.5.

of defectively coordinated atoms. Such an increase indeed favours the coalescence between different clusters and thus a net decrease in N_{cl}.

The defectively coordinated atoms form aggregates of various shape and size, similar to those observed in the case of fcc and hcp metals. The clusters occasionally display the configurations that are typical of dislocations and point defects. It is worth noting that the dislocations that are detected undergo displacements roughly in agreement with the slip systems of the bcc lattice. In particular, dislocations with (110) and (211) glide planes are seen to move approximately along the [111] crystallographic direction.

3.4. Elements with bcc structure

On the basis of the findings presented above, elements with the bcc structure are expected to display a melting behaviour that is significantly different from those of the fcc and hcp systems. The origins of such differences can reasonably be ascribed to the fact that, contrary to both the hcp and fcc structures, the bcc lattice is not close-packed.

The fraction $\alpha_d(T)$ of defectively coordinated atoms for the two bcc metallic species is shown in figure 9(a) as a function of the reduced temperature T/T_m^K. The data of Mo and V arrange according to superposed monotonic trends pointing out $\alpha_d(T_m^K)$ values at the homogeneous melting point T_m^K of about 0.5. This value is the same as those observed in the cases of the Ti and Zr systems melting with the bcc structure.

The number N_{cl} of defectively coordinated atom clusters is reported in figure 9(b) as a function of the reduced temperature T/T_m^K. The curves of Mo and V are again superposed.

The HA analysis of the local crystalline order points out the formation of domains of about 20 atoms with hcp arrangement. Finally, the observed dislocations move on (110) and (211) glide planes approximately along the [111] crystallographic direction.

4. Discussion

The numerical findings concerning both the fraction $\alpha_d(T)$ of defectively coordinated atoms and the number N_{cl} of the clusters that they form are summarized in figures 10(a) and (b), where the data of the different systems are quoted as a function of the reduced temperature

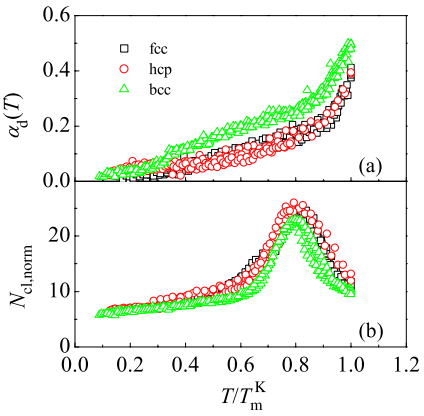

Figure 10. The fraction $\alpha_d(T)$ of defectively coordinated atoms (a) and the normalized number $N_{cl,norm}$ of clusters of defectively coordinated atoms (b) as a function of the reduced temperature T/T_m^K for the 11 metals investigated. The compact fcc and hcp structures display $\alpha_d(T)$ and $N_{cl,norm}$ values that are larger and smaller, respectively, than those pertaining to bcc elements.

T/T_m^K. Due to the hcp-to-bcc phase transition undergone by Ti and Zr, part of their data is reported as hcp and part as bcc.

It can be seen from figure 10(a) that the curves of the elements with compact structures group together, as well as those of the elements melting with a bcc structure. It also appears that the limit of superheating, T_m^K, represents a scaling factor for all the elements investigated. The elements that melt with either fcc or hcp lattices display $\alpha_d(T_m^K)$ values on the order of 0.4, whereas the species that melt with a bcc structure display $\alpha_d(T_m^K)$ values of about 0.5. This evidence suggests that the fraction $\alpha_d(T_m^K)$ of defectively coordinated atoms at the limit of superheating, T_m^K, is a quantity that is characteristic of the geometry of the crystalline lattice.

The larger fraction $\alpha_d(T)$ of defectively coordinated atoms observed in bcc systems is at the origin of the smaller number N_{cl} of clusters that they contain. The number of clusters normalized to the total number of atoms in the system, $N_{cl,norm}$, is quoted in figure 10(b) as a function of the reduced temperature T/T_m^K. As in the previous case, the data of the elements group together in dependence of the crystalline lattice with which the element melts. The cumulative curve of the bcc elements is always lower than those pertaining to the compact structures.

These findings suggest that the geometry of the crystalline lattice undergoing a gradual temperature rise has a fundamental role in the mechanism determining the final collapse at the limit of superheating. Such behaviour is not surprising in the light of the existing experimental, theoretical and numerical studies [3, 42]. For example, it is a well-known fact that heterogeneous melting and correlated pre-melting phenomena are strongly sensitive to the surface structure [2, 3, 36, 38, 39, 42, 43]. Surfaces with different Miller indexes display different pre-melting and heterogeneous melting points [2, 3, 42, 43]. Despite the evident and expected dependence on the structure, universal behaviours can however be identified [2, 6, 17, 40]. Even though the conceptual framework has not been understood yet, such behaviours can be ascribed to the interplay between structure and dynamics. Both experimental and numerical evidence, for example, concur to point out a deep connection between the volume available to atomic species, relative mobility, mechanical properties and melting point [2, 3, 42]. In a sense, the numerical findings discussed in the present work agree with such evidence, given that the largest fraction of defectively coordinated atoms is observed not in the close-packed lattices but in the more open bcc structures. However, a definite

relationship between structure and melting behaviour has not been found yet and a systematic experimental and numerical investigation of the heterogeneous and homogeneous melting processes is necessary to advance the basic knowledge in the field further. The accomplishment of such a task is also necessary in the light of the deep differences between heterogeneous and homogeneous solid–liquid transitions [2, 3, 7, 8, 40]. In the former case, the failure of the crystalline phase is due to the large mobility of surface species and this, in turn, is connected with the topology of the crystalline plane that is exposed [42]. Surface reconstructions further complicate the problem [42]. The heterogeneous melting process gradually involves the bulk starting from surfaces and interfaces, whereas homogeneous melting immediately involves the whole bulk. However, careful study of the heterogeneous melting features is expected to throw light on the mechanism of homogeneous melting [8], which however does not change substantially with the crystalline lattice geometry. In all the cases, it is intimately related to the proliferation of defects in the bulk.

The proliferation of atoms with defective coordination in the bulk determines a significant increase in the atomic mobility, particularly in the superheating regime. According to the observations mentioned above, this can be considered as the fundamental reason for the lattice failure. The atoms with defective coordination indeed leave the equilibrium lattice positions and compromise the mechanical stability of the crystalline lattice. Atomic displacements take place according to a cooperative mechanism, the features of which recall previous studies [44, 45]. The atoms indeed move along string-like paths that can be regarded as alternative routes to thermally activated interdiffusion [46]. However, further investigations along this line are necessary to characterize fully the nature of the clusters of defectively coordinated atoms assisting the atomic displacements and determine the role of interstitials, as predicted in previous work [44].

5. Conclusions

The systematic study of the thermal response to a gradual temperature rise of crystalline lattices with different geometry has shown that homogeneous melting at the limit of superheating is governed by the formation of atoms with defective coordination. The calculations performed indicate that the amount of defectively coordinated atoms at the failure of the crystalline structure is intrinsically dependent on its geometry. The fraction of defectively coordinated atoms is then characteristic of the lattice geometry. This evidence establishes a definite connection between lattice topology and the melting mechanism. Further work is necessary in order to throw light on the reasons underlying the different characteristic values of the fraction of defectively coordinated atoms, as well as on the actual role of lattice defects. A careful characterization of heterogeneous melting mechanisms is also necessary to gain deeper insight into the role of the lattice topology in both heterogeneous and homogeneous solid–liquid transition processes.

Acknowledgments

Financial support has been provided by the University of Cagliari. Professor G Cocco, Dipartimento di Chimica, Università degli Studi di Sassari, is gratefully acknowledged for useful discussions. A Ermini, ExtraInformatica s.r.l., is gratefully acknowledged for technical support.

References

[1] Stillinger F H and Weber T A 1984 *Science* **228** 983
[2] Kleinert H 1989 *Gauge Theory in Condensed Matter* (Singapore: World Scientific)

[3] Dash J G 2002 *Contemp. Phys.* **43** 427
[4] Tallon J L 1989 *Nature* **342** 658
[5] Born M and Huang K 1954 *Dynamical Theory of Crystal Lattices* (Oxford: Clarendon)
[6] Lu K and Li Y 1998 *Phys. Rev. Lett.* **80** 4474
[7] Jin Z H *et al* 2001 *Phys. Rev. Lett.* **87** 055703
[8] Cahn R W 2001 *Nature* **413** 582
[9] Lindemann F A 1910 *Phys. Z.* **11** 609
[10] Gilvarry J J 1956 *Phys. Rev.* **102** 308
[11] Gomez L *et al* 2003 *Phys. Rev. Lett.* **90** 095701
[12] Delogu F 2006 *Mater. Sci. Eng.* A **416** 33
[13] Delogu F 2006 *J. Phys. Chem.* B **110** 3281
[14] Gomez L *et al* 2005 *Phys. Rev.* B **71** 134106
[15] Cotterill R M J 1979 *Phys. Rev. Lett.* **42** 1541
[16] Cotterill R M J 1980 *Ordering in Strongly Fluctuating Condensed Matter Systems* (*NATO-ASI Series B* vol 50) ed T Riste (New York: Plenum) pp 261–6
[17] Burakovsky L *et al* 2000 *Phys. Rev.* B **61** 15011
[18] Kosterlitz J M and Thouless D J 1973 *J. Phys. C: Solid State Phys.* **6** 1181
[19] Nelson D R and Halperin B I 1979 *Phys. Rev.* B **19** 2457
[20] Young A P 1979 *Phys. Rev.* B **19** 1855
[21] Cahn R W and Haasen P (ed) 1996 *Physical Metallurgy* 4th revised and enhanced edn (Amsterdam: Elsevier Science BV)
[22] Ducastelle F 1970 *J. Physique* **31** 1055
[23] Rosato V *et al* 1989 *Phil. Mag.* A **59** 321
[24] Cleri F and Rosato V 1993 *Phys. Rev.* B **48** 22
[25] Finnis M W and Sinclair J E 1984 *Phil. Mag.* A **50** 54
[26] Daw M S and Baskes M I 1983 *Phys. Rev. Lett.* **50** 1285
[27] Daw M S and Baskes M I 1984 *Phys. Rev.* B **29** 6443
[28] Haberland H *et al* 1995 *Phys. Rev.* B **51** 11061
[29] Sorkin V *et al* 2003 *Phys. Rev.* B **68** 174103
[30] Allen M P and Tildesley D 1987 *Computer Simulation of Liquids* (Oxford: Clarendon)
[31] Andersen H C 1980 *J. Chem. Phys.* **72** 2384
[32] Nosè S 1984 *J. Chem. Phys.* **81** 511
[33] Brandes E A and Brook G B (ed) 1992 *Smithells Metals Reference Handbook* 7th edn (Oxford: Butterworth-Heinemann)
[34] Honeycombe R W K 1985 *The Plastic Deformation of Metals* (London: Edward Arnold)
[35] Phillpot S R *et al* 1989 *Phys. Rev.* B **40** 2831
[36] Wolf D *et al* 1990 *J. Mater. Res.* **5** 286
[37] Honeycutt J D and Andersen H C 1987 *J. Phys. Chem.* **91** 4950
[38] Lutsko J F *et al* 1989 *Phys. Rev.* B **40** 2841
[39] Rosato V *et al* 1986 *Phys. Rev.* B **33** 1860
[40] Delogu F 2006 *Phys. Rev.* B **73** 184108
[41] Willaime F and Massobrio C 1989 *Phys. Rev. Lett.* **63** 2244
[42] Tartaglino U *et al* 2005 *Phys. Rep.* **411** 291
[43] Sheng H W *et al* 1998 *Acta Mater.* **46** 5195
[44] Nordlund K *et al* 2005 *Europhys. Lett.* **71** 625
[45] Donati C *et al* 1999 *Phys. Rev.* E **60** 3170
[46] Delogu F 2005 *J. Phys. Chem.* B **109** 15291